Relative Distance Estimation for Indoor Multi-robot Control Using Monocular Digital Camera

Ying-Hao Yu, Sarath Kodagoda, and Q.P. Ha

School of Electrical, Mechanical and Mechatronic Systems,
University of Technology, Sydney
PO Box 123, Broadway, NSW 2007 Australia
E-mail: {YingHao.Yu, Sarath Kodagoda, quangha}@eng.uts.edu.au

Abstract

Distance measurement methodologies based on the digital camera usually require extensive calibration routines, some are even derived from complicated image processing algorithms resulting in low picture frame rates. Particularly, in a dynamic camera system, due to the unpredictability of intrinsic and extrinsic parameters, the reliable measuring results are highly dependent on the accuracy of extra sensors. In this paper, a simple algorithm for relative distance estimation is proposed for multi-robot control with a monocular digital camera. Reasonable accuracy is achieved by judging the 2D perspective projection image ratio (PPIR) of robots' labels on a TFT-LCD (Thin Film Transistor–Liquid Crystal Display) monitor without any additional sensory cost and complicated calibration effort. Further, the algorithm does not contain any trigonometric functions so that it can be easily implemented on an embedded system using the field programmable gate array (FPGA) technology.

1. Introduction

For relative distance measurement and localisation in a multiple robot system, the use of laser range finders [1], ultrasonic sensors [2] and communication networks [3] is quite popular. Laser range finders and ultrasonic sensors use the concept of time-of-flight (TOF) to measure the relative distance between two robots. In communication networks, distance measurement requires a routing time and also reception of a radio signal strength indication (RSSI). The robot will then be able to approximate relative distances by judging the attenuation of radio strength from adjacent objects [4]. Although these sensors are feasible for range measurement, there are few disadvantages of using them due to the limited information content. For example, they may not be able to comprehensively understand and model the operating environment. In contrast, digital cameras seem to be more versatile by having a large amount of information in terms of texture, colour, illumination, edges, optical flows, distance, etc. Further, while the use of laser, ultrasonic, and radio signals may be limited by active interferences due to crowded sensors, the camera, being a passive sensor, has no such limitation.

Recently, the combination of infrared (or laser) and digital camera sensors is reported as a feasible technology for distance measurement by using a time-of-flight measurements (TOF) camera. It measures the traveling time of the reflected light between the camera and the target. This distance is then presented in a depth map [5]. Unfortunately, these kinds of camera designs usually have disadvantages in a low dynamic range of depth maps, high power consumption for active illumination with LEDs, and computational complexity [6]. Therefore, they are generally not considered in the design of embedded systems in ubiquitous robotics [7].

In spite of possible power capacity improvements via new components and battery technologies in the future, the real-time computation has become an issue in using wireless communication networks [8], where the external server needs to accommodate the computation requirements. This can lead to other problems due to inherent bottlenecks of networks' data throughput and security problems. Consequently, in recent years, global camera systems with onboard computation [9] are increasingly popular in distance measurement. For a fixed camera set up, it is possible to determine the distance to an object based on optical properties [10] as:

$$\frac{1}{x}+\frac{1}{y}=\frac{1}{f} \tag{1}$$

$$\frac{h}{h'}=-\frac{x}{y}, \tag{2}$$

where x is the distance far from the camera lens with height h of a perpendicular object, f is the focus of camera's lens, and y is the image distance to lens with relative pixel height h' on the camera's digital sensor array. In practical applications, (1) and (2) can also be modified for real-world applications such as obstacle detection in smart car systems [11]. A convenient technique was proposed for comparing the variant dimension of image by shifting camera's position on a straight line [12].

For indoor robot navigation, where the floor is assumed to be flat, it is possible to utilise markers or labels as visual features [13]. For that, a label may be attached onto the robot to be detected by a global camera system without modifying the indoor facility [14]. However, depending on where the camera is mounted, scene interpretation and depth calculation may involve complicated expressions, as illustrated in Fig. 1. Therein, the distance between robots is obtained by a trigonometric equation:

$$d = h[\tan(\theta_0 + \tan^{-1}\frac{y_0^{'} + d^{'}}{p}) - \tan(\theta_0 + \tan^{-1}\frac{y_0^{'}}{p})], \quad (3)$$

where, h is the installation height of camera's lens, p is the projected image distance from the image sensor array to lens, y_1 and y_0 are the label lengths of leading and following robots, the relative distance between the two robots is d, and the lengths of images on a digital image sensor array are respectively $y_1^{'}$, $d^{'}$, and $y_0^{'}$. Although the distance given in (3) is a feasible solution, in a dynamic camera system, the height of camera and the camera's tilting angle θ_0 are usually changing. Further, the focal length of the camera might be unknown. Those issues can be overcome by integrating additional sensors and choosing high-end cameras. However, the hardware risk may also occur with all uncertainties of additional sensory readings.

In this paper, we propose a new relative distance measurement algorithm for monocular cameras, based on the digital photography framework [15]. By detecting the 2D labels on the top of indoor robots, the algorithm can estimate the relative distance between robots by calculating the perspective projection image ratio (PPIR) of labels, similarly to human perception but with a higher accuracy. This algorithm can estimate the relative distance of robots under various dynamic conditions such as unknown tilt angle, height to lens, and focal length of the camera without recalibrating or mounting extra sensors. Further, we also consider a simple implementation of the algorithm in an embedded system using the FPGA technology [16] by avoiding all complicated expressions including trigonometric or exponential functions.

The paper is organised as follows. In the second section, the proposed PPIR algorithm is introduced, and the test schemes and results are presented in Section 3. Discussion is given in Section 4. Finally, a conclusion is drawn in the last section.

2. The PPIR Algorithm

It is assumed that the 2D circle labels are fixed on top of robots and the floor is flat. Estimated distances in lateral and longitudinal are discussed separately in the following subsections.

2.1. Estimation of longitudinal distance based on PPIR

Figure 2(a) shows a sketch of deployment of robots (labels) in real world coordinates with a leading robot (label length y_1) and a following robot (label lengh y_0) which are separated by a distance d in longitudinal direction. The imagined perspective image of robots' on the TFT-LCD monitor are shown on the Fig. 2(b) with the unknown tilted angle and focus of the camera.

To find the real relative distance d by utilising the perspective image on the TFT-LCD monitor, the distance is then translated into a ratio between relative distance and robots' label lengths, which can be expressed as:

$$\frac{d^{'}}{y_0^{'}} \le \frac{d}{y_0} \le \frac{d^{'}}{y_1^{'}}, \text{ and } y_0 = y_1 \quad (4)$$

where $y_0^{'}$, $y_1^{'}$, and $d^{'}$ represent respectively the relative perspective length of the follower, leader, and relative distance on the TFT-LCD monitor. Consequently, if both robots are very close to each other or the camera is perpendicularly oriented to the floor, the real distance can be estimated by the average of perspective label lengths:

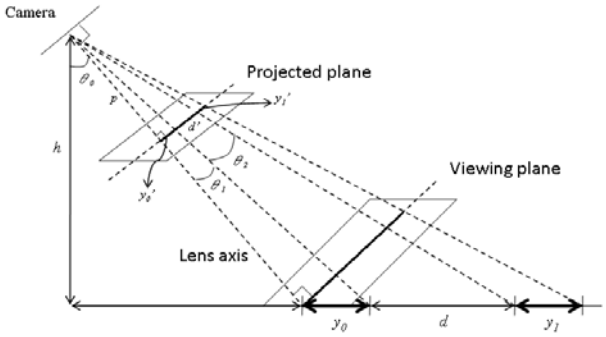

Fig. 1 An example of image projection in a global camera system with 2D label in single direction view, where y_1 and y_0 are the label lengths of leading and following robots respectively.

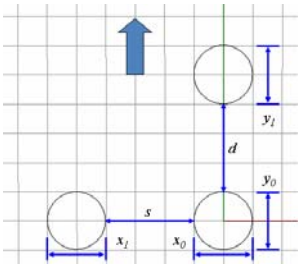

a. The real robots' deployment presented in circles.

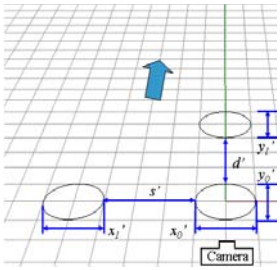

b. The perspective view in real world.

Fig. 2 Different views between real deployed robots and their persepctive image.

$$\frac{d}{y_0} \cong \frac{1}{2}\left(\frac{d^{'}}{y_0^{'}} + \frac{d^{'}}{y_1^{'}}\right). \quad (5)$$

In real operations, (5) will result in an intolerable error when the leader is moving further away, because the fast decreasing label length of the leader will be

dominant, thus yielding a large positive error. Therefore, by combining the equations in (5) and (4), a new upper limit of (4) can be derived as:

$$\frac{d}{y_0} \le \frac{1}{2}\left(\frac{d'}{y_0'} + \frac{d'}{y_1'}\right). \tag{6}$$

The lower limit can be also approximated by a ratio $\delta_y = y_1'/y_0'$

$$d'\left(\frac{y_0'+y_1'}{2y_0'y_1'}\right)\cdot\delta_y \le \frac{d}{y_0}. \tag{7}$$

To prove the relationships of (6) and (7), we can translate the perspective image as :

$$y_0' = ky_0 \text{ , and } y_1' = \lambda y_0 \tag{8}$$

here, $\lambda \le k \le 1$, so the assumption in (6) and (7) can be demonstrsted by an approximated trapezoid area:

$$d' = \frac{R_v(\lambda y_0 + k y_0)}{2}\times\eta, \tag{9}$$

where R_v denotes the ratio of d/y_0, and $1 \le \eta < 2$.

Now by substituting

$$\frac{d'}{y_0'} = \frac{R_v(\lambda+k)}{2k}\times\eta, \tag{10}$$

and

$$\frac{d'}{y_1'} = \frac{R_v(\lambda+k)}{2\lambda}\times\eta, \tag{11}$$

into (5), we have

$$\frac{1}{2}\left(\frac{d'}{y_0'} + \frac{d'}{y_1'}\right) = \frac{R_v\eta(\lambda+k)^2}{4k\lambda} \ge \frac{d}{y_0}. \tag{12}$$

This verifies the upper limit in (6). The lower limit can also be derived as:

$$\frac{R_v\eta(\lambda+k)^2}{4k\lambda}\frac{\lambda y_0}{k y_0} = \frac{R_v\eta(\lambda+k)^2}{4k^2} \le \frac{d}{y_0} \tag{13}$$

So the new estimated distance range is rewriten as:

$$d'\left(\frac{y_0'+y_1'}{2y_0'y_1'}\right)\cdot\delta_y \le \frac{d}{y_0} \le d'\left(\frac{y_0'+y_1'}{2y_0'y_1'}\right) \quad . \tag{14}$$

Here we redefine the real relative distance ratio in longitudinal direction as:

$$\frac{d}{y_0} = R_v \cong d'\left(\frac{y_0'+y_1'}{2y_0'y_1'}\right)\cdot\delta_v,\ \delta_y \le \delta_v \le 1 \tag{15}$$

To find the constant δ_v, the following converging series leads to the approximation:

$$\delta_v = \delta_y + \sum_{n=1}^{n=\infty}\frac{1}{2^n}(1-\delta_y) \cong \frac{(2^n-1)y_0'+y_1'}{2^n y_0'}. \tag{16}$$

According to our experiments by using several generic digital cameras, the reasonable value for δ_v is obtained when n is between 3 and 4 for an expected tolerance less than 5% of the real distance.

By observing (16), it can be seen that variable δ_v can be adjusted automatically without requiring any additional optical installation or information of the camera. Particularly, when both robots are found closely to each other or the camera has a zero tilt angle, the leader's label length y_1' will converge to the label length of the follower, y_0'. This makes δ_v approach 1, and therefore (15) is simply brought to (5).

2.2. PPIR Estimation of Lateral Distance based on PPIR

In the robotic deployment with a lateral displacement, shown in Figure 2, the leader is moving parallel to a follower on the left side. The label width of the leader, follower, and relative distance in real world coordinates are denoted as x_1, x_0 , and s as in Fig. 2(a). Meanwhile, the relative parameters of the perspective image are x_1' , x_0', and s', as given in Fig. 2(b).

The relative distance in lateral direction can be found by using a similar algorithm. However, due to the image beyond the central line of camera's lens (or TFT-LCD monitor) is twisted by a perspective phenomenon, the image of the leader will be a little bit wider than its follower (Fig. 2(b)). Correspondingly, variable δ_x can be redefined as x_0'/x_1'. Now it can be shown that,

$$s'\left(\frac{x_0'+x_1'}{x_0'x_1'}\right)\cdot\delta_x \le \frac{s}{x_0} \le s'\left(\frac{x_0'+x_1'}{2x_0'x_1'}\right), \tag{17}$$

where

$$\frac{s}{x_0} = R_h \cong s'\left(\frac{x_0'+x_1'}{2x_0'x_1'}\right)\cdot\delta_h. \tag{18}$$

Finally, we also have with $\delta_x \le \delta_h \le 1$:

$$\delta_h = \delta_x + \sum_{n=1}^{n=\infty} \frac{1}{2^n}(1-\delta_x) \cong \frac{(2^n-1)x_1' + x_0'}{2^n x_1'}. \quad (19)$$

2.3 Estimation of Euclidean Distance based on PPIR

Consider now the generic case of a triangular robotic formation, where the hypotenuse distance is obtained as:

$$R_s = \sqrt{R_v^2 + R_h^2}. \quad (20)$$

However, it may not be ready to determine the PPIR horizontal distance R_h due to the unavailability of the lateral label width of follower. Here, a virtual width x_t located at the image centre is adopted for x_0 in (17-19) as:

$$x_t = x_0 = \alpha x_1, \quad (21)$$

where α is decided empirically such that the average error is less than 5% at any reasonable operational location in a half plane.

3. Experimental Results

The rigid circles (labels) are installed horiziontally on top of the Eyebots, miniature mobile robots with same height. For convenience of computing, the circular discs are cut with 10cm of diameter and the separation distance is set to 1m. The "blue" colour is chosen for the labels to improve the contrast. The general camera is used with 5M pixel resolution and an adjustable focus from 7.1 to 21.4 mm. The changing of focal length is judged by reading the relative adjustable aperture range from f2.8 to f4.8. Constant α is set at 0.95.

A one-time calibration is then performed. The robots' perspective images are measured by a digital caliper. Fig. 3 shows some of tested schemes with PPIR algorithm. From Fig. 3(a) to (e), the images with the same longitudinal deployment are captured randomly by different tilted angles, installation heights, and focuses. In Fig. 3(f), a basic triangular layout in the left plane is shown for simulating a formation scenario, where the robot located on the left-top corner represents the leading robot and the follower located at the bottom. The robot at the middle represents the virtual robot included here to verify the selection of constant α.

The estimation results about choosing the degree n for values of δ_v and δ_h in (16) and (19) are demonstrated in the Table 1. When n = 3, the PPIR estimation has negative error while the positive error is observed with n = 4. The criterion of measruing error is defined by the difference between real, 100cm and 141.5cm, and the estimated distance in percent.

In summary, Table 1 has demonstrated the accuracy of PPIR in relative distance measurements even in all cases. The value n=3 yields a satisfactory expectation of less than 5% in error.

Table. 1 The tested results of PPIR estimation, δ_v and δ_h are designed with different degrees of n as in Fig. 3.

Tests	Real Distance (cm)	Error n = 3 (%)	Error n = 4 (%)	Average Error n = 3 & 4 (%)
(a)	100	-0.95	+1.93	+0.49
(b)	100	-3.37	+0.58	-1.4
(c)	100	-3.17	+1.6	-0.78
(d)	100	-2.3	+1.31	-0.49
(e)	100	+4.7	+9.72	+7.21
(f)	141.5	+0.05	+2.36	+1.2

4. Discussion

Observing the test results in Table 1, it can be seen that the PPIR algorithm can acceptably estimate the relative distance by simply using the perspective image changing ratio between robots (labels). Moreover, the proposed technique can track the real changing curve of the perspective distance without involving any complicated mathematical functions. In reference to (3), computation time can be significantly reduced even without using a look-up table in memory, as suggested in [17]. Notably, the results are not much affected by the camera parameters. Within a reasonable working range, n = 3 is suitable for cameras used for a relatively large monitoring area while n = 4 gives a higher accuracy at near locations.

Another important contribution of the PPIR algorithm is that estimation results are insensitive to the camera focus. From Fig. 3 and Table 1, it can be seen that the PPIR still keeps its accuracy when the camera's focus is changed (variant aperture readings). Hence, even the PPIR algorithm is only tested with the indoor robots in a narrow space, it can also be used with changing views with adjusted focus for high quality imaging.

The label desgined as a circle leads to an elliptical shape in the perspective to better illustrate the derivation of the relative distance in both lateral and longitudinal directions. For different object sizes (robots), the dual circles in a concentric design may be used. After estimating the PPIR distance for the inner circle, the relative distance with various dimensions of circles (robots) can be obtained by deducting the difference of radii from the PPIR distance.

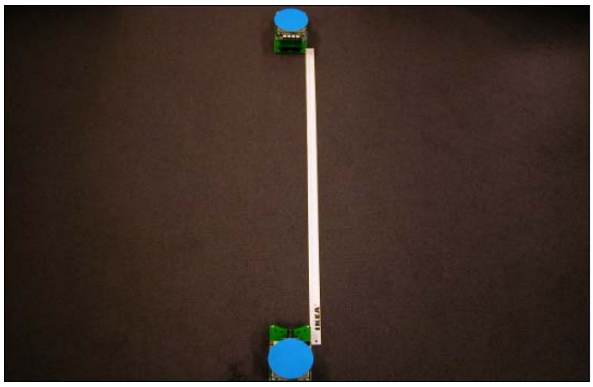

(a)Camera height: 130cm / tilted angle: 10^{o} / aperture: f2.8.

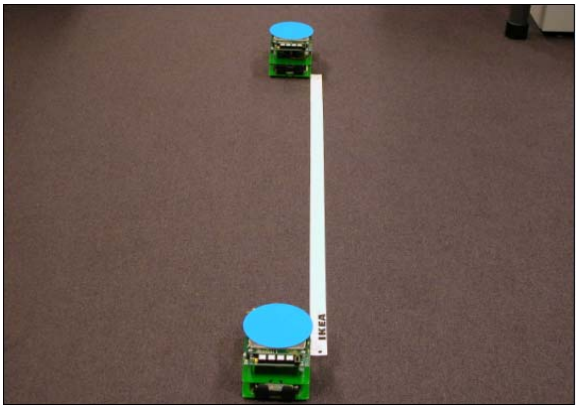

(b) Camera height: 111cm/ tilted angle : 30^{o}/ aperture: f4.0.

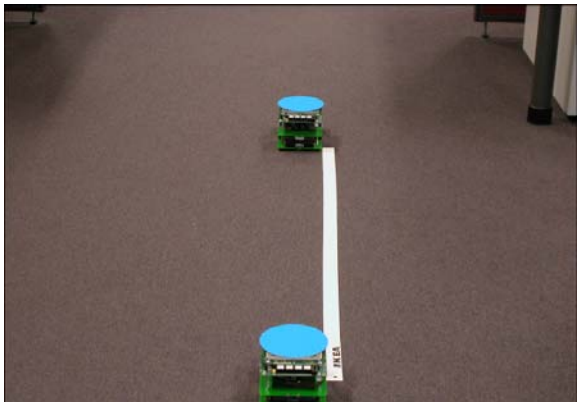

(c) Camera height: 111cm/ tilted angle : 75^{o}/ aperture: f4.8.

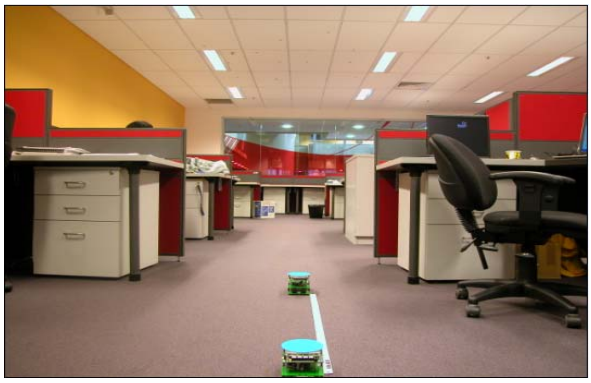

(d) Camera height: 51cm/ tilted angle: 90^{o}/ aperture: f2.8.

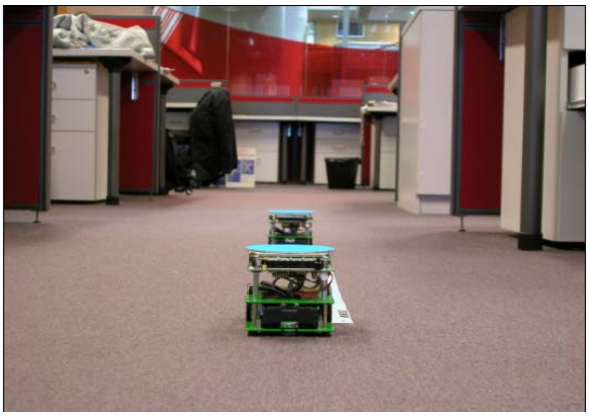

(e) Camera height: 19cm/ tilted angle: 90^{o}/ aperture: f4.0.

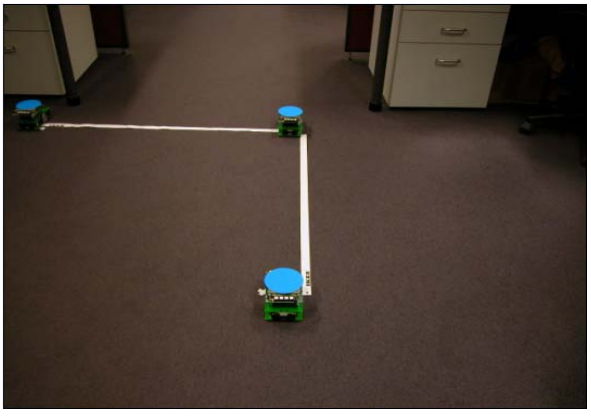

(f)Camera height: 112cm/ tilted angle: 30^{o}/ aperture: f2.9.

Fig. 3. Different scenarios for testing.

5. Conclusion

In this paper we have proposed a new relative distance measurement algorithm for multi-robot systems with least calibration and computation efforts. Unlike the conventional distance measurement techniques, where the low dynamic range of depth map, complicated image algorithms, and high power consumption for active illumination may make the time-of-flight methodology unsuitable for compact indoor robot design. In contrast, the PPIR algorithm with a single digital camera is immune to these mentioned concerns. By observing the labels on mobile indoor robots, the proposed PPIR algorithm calculates the relative distance accurately and instantly with different ratios between perspective labels and distance images. Simplicity in the algorithm derivation makes it promising for implementation with by the field programmable gate array (FPGA) technology for indoor multi-robot formation control.

References

[1] N. Trawny, X.S. Zhou, and K.X. Zhou, and S.I. Roumeliotis, "3D Relative Pose Estimation from Distance-Only Measurements", *IEEE Intl. Conf. on Intelligent Robots and Systems*, San Diego, USA, 2007, pp. 1071-1078.

[2] M.K. Lee, J.O. Park, and J.E.S. Song, "User Authentication Based on Distance Estimation Using Ultrasonic Sensors", *IEEE Intl. Conf. Computation Intelligence and Security*, Suzhou, China, 2008, pp. 391-394.

[3] C.Y. Wen, R.D. Morris, and W.A. Sethares, "Distance Estimation Using Bidirectional Communications Without Synchronous Clocking", *IEEE Trans. on Signal Processing*, 2007, Vol. 55, No. 5, pp. 1927-1939.

[4] W. Xiao, Y. Sun, Y. Liu, and Q. Yang, "TEA: Transmission Error Approximation for Distance Estimation between Two Zigbee Devices", *IEEE Intl. Conf. Networking, Architecture, and Storage*, Shenyang, China, 2006, pp. 15-22.

[5] J.M. Dubois and H. Hüglí, "Time-of-flight imaging of indoor scenes with scattering compensation", *Proc. of the 8th Conference on Optical 3-D Measurement Techniques*, Zurich, Switzerland, 2007, pp. 117-122.

[6] H. Rapp, *Experimental and Theoretical Investigation of Correlating TOF-Camera Systems*. University of Heidelberg, pp. 59-63, Germany, 2007.

[7] J.H. Kim, "Ubiquitous Robot: Recent Progress and Development", *Proc. IEEE/ SICE Intl. Conf Digital Object Identifier*, Busan, Korea, pp. 25- 30, 2006.

[8] Y.Y. Li , W.R. Fan, Y.R. Liu, and X.P. Cai, "Teleoperation of Robots via the Mobile Communication Networks", *IEEE Intl. Conf. Robotics and Biomimetics*, Hong Kong, 2005, pp.670-675.

[9] A. Stubbs, V. Vladimerou, A.T. Fulford, D. King, J. Strick, and G.E. Dullerud, "Multivehicle Systems Control over Networks: a hovercraft testbed for networked and decentralized control", *IEEE Control System Magazine,* Vol. 26. No. 3, pp. 56-69, 2006.

[10] Q. Chen, F. Tan, and P.Yung. Woo, "An Improved Distance Measurement Method for Four-Legged Robots Based on the Colour Region", *Proc. IEEE Intl. Conf. on Intelligent Control and Automation*, Chongqing, China, 2008, pp. 3040-3044.

[11] J. Chang and C.W. Cho, "Vision-Based Front Vehicle Detection and Its Distance Estimation", *IEEE Intl. Conf. on System, Man, and Cybernetics*, Taipei, Taiwan, 2006, pp. 2063-2068.

[12] N. Yamaguti, O.E. Shunichiro, and K. Terada, "A Method of Distance Measurement by Using Monocular Camera", *IEEE Intl. Conf. SICE'97*, Tokyo, Japan, 1997, pp.1255-1260.

[13] R.D. Andrea and P. Wurman, and W. P, "Future challenges of coordinating hundreds of autonomous vehicles in distribution facilities", *IEEE/ TePRA Intl. Conf on Technologies for Practical Robot Application*, Woburn, USA, pp. 80-83, 2008.

[14] V. Vladimerou, A. Stubbs, J. Rubel, A. Fulford, J. Strick, and G.E. Dullerud, "A hovercraft testbed for decentralized and cooperative control", *Proc. American Control Conf.*, Vol. 6., pp. 5332-5337, 2004.

[15] M. Galer, *Digital Photography in Available Light*. Elsevier, UK, 2006, pp. 224.

[16] Y.-H. Yu, N.M. Kwok, and Q.P. Ha, "FPGA-Based Real-Time Color Tracking for Robotic Formation Control," *Proc. of the Int. Conf. Robotics and Automation in Construction*, Austin, USA, pp. 252-258, 2009.

[17] J.-P. Deschamps, G.J.A. Bioul, and G.D. Sutter. *Synthesis of Arithmatic Circuits*. John Wiley & Sons, Canada, 2006.